

## Decision-Aided Extended Kalman Filter Based Adaptive Timing Recovery for Wavelet Packet Modulated Signals\*

SUN Yi (孙懿), HAO Jiuyu (郝久玉)\*\*

School of Electronic Information Engineering, Tianjin University, Tianjin 300072, China

**Abstract:** One of the major issues with multi-carrier systems is their vulnerability to timing synchronization errors resulting in the loss of time synchronization which causes loss of orientation of incoming data at the receiver. This paper presents an acquisition algorithm to timing recovery using the decision-aided extended Kalman filtering (EKF) technique for nonlinear disturbance channels in a wavelet packet transform-based multicarrier modulation communication system. This timing recovery algorithm gives faster convergence, smaller root mean square (RMS) errors, and better bit error rate (BER) performance than traditional timing recovery methods, such as the phase-locked loop (PLL), maximum likelihood (ML), and Kalman filter (KF) methods. Thus, the algorithm is able to handle larger timing errors more reliably and to provide better timing recovery, since the scheme takes into account the nonlinear relationship between the signal samples and timing errors. Simulations for various time-varying channels show that the timing recovery algorithm works well for wavelet packet transform-based multicarrier modulation communication systems.

**Key words:** wavelet packet transform; multi-carrier modulation; adaptive timing recovery; extended Kalman filter

### Introduction

Multi-carrier modulation (MCM) is an efficient spectral modulation scheme which is robust against channel dispersions/fading, impulse noise, and multipath interference. Wavelet packet modulation (WPM) is an MCM technique that has recently emerged as a strong candidate for digital modulation as an alternative to orthogonal frequency division multiplexing (OFDM)<sup>[1]</sup>. However, one major issue with multi-carrier systems is their vulnerability to timing synchronization errors resulting in a loss of time synchronization which

causes a loss of orientation of incoming data at the receiver. The fundamental theories of OFDM and WPM have many similarities in their functioning and performance but there are some significant differences which give the two systems distinctive characteristics<sup>[2]</sup>. OFDM signals only overlap in the frequency domain while the wavelet packet signals overlap in both the time and frequency domains. Due to the time-overlap, the WPM system can not use the cyclic prefix (CP) or any kind of guard interval (GI) that is commonly used to overcome interference caused by dispersive channels in OFDM systems. Thus, the methods for correcting time synchronization errors originating from symbols misalignment at the demodulator of the OFDM system are not suitable to the WPM system.

This paper investigates how a WPM system utilizing known wavelets and time recovery techniques can cope with synchronization errors and how their

---

Received: 2009-08-03; revised: 2010-03-19

\* Supported by the Tianjin Natural Science Foundation in China (No. 043600611) and the Science and Technique Fostering Foundation of Tianjin in China (No. 043102911)

\*\* To whom correspondence should be addressed.

E-mail: hao1945@eyou.com; Tel: 86-22-87893287

performance compares with that of OFDM.

In recent years, a number of time recovery approaches have been developed. For example, the recursive discrete Fourier transform (RDFT) method synthesizes a unitary synchronizing signal using the RDFT information, independent of the conditions. However, the RDFT frequency estimation dynamics are not smooth. In addition, there is no direct three-phase version of the RDFT method and it needs an amplitude detector if the frequency deviates from the nominal value<sup>[3]</sup>. The conventional PLL may fail to correct initial errors in acquisition due to its limited bandwidth<sup>[4]</sup>. A popular approach for time recovery is the maximum likelihood decision-directed (MLDD) method where an appropriate likelihood function is maximized with no assumptions about a priori probability densities. One of disadvantages of the MLDD method is that an extensive search may be required to find the optimal estimate when the density function has several peaks and that the favorable properties, the unbiasedness and consistency of the estimates, do not necessarily hold if the unknown quantity is actually time varying<sup>[5]</sup>. A timing recovery approach based on Kalman filtering has been proposed in order to improve timing recovery performance. However, earlier works are based on a linear model of the relation between the receiving signal and timing offset when the relation is actually nonlinear<sup>[3,6]</sup>.

In general, timing recovery in communication systems uses an acquisition stage and a tracking stage. This paper focuses on the acquisition stage with an adaptive timing recovery algorithm using a decision-aided EKF which explicitly includes the nonlinear relationship between the received signal and the timing offset which is applied to a wavelet packet transform-based multicarrier modulation communication system. Simulations for an additive white Gaussian noise (AWGN) channel and a Rayleigh fading channel model are used to evaluate the performance of this approach compared to conventional timing recovery methods. Although the overall complexity of an EKF scheme timing estimate is quite a bit larger than conventional methods since the Kalman gains vary with time, these gains can be pre-computed offline. This method then converges faster than conventional PLL, ML or KF based timing recovery methods.

## 1 Nonlinear Disturbance System Model

Assume  $\mathbf{u}_k$  represents a transmitted sequence which passes through a time-varying, frequency selective fading channel,  $\mathbf{y}_k$  is the multiplicative distortion (MD),  $\mathbf{v}_k$  is a discrete-time AWGN, and  $\mathbf{z}_k$  is the received signal. The transmitted signals suffer from time, phase, and frequency offsets resulting from the MD due to the time-varying, frequency selective fading channel. The goal of a general “timing synchronizer” is to provide a good estimate of the MD,  $\mathbf{y}_k$ , which may include the phase/frequency errors of the mixers and time-varying amplitudes and phases introduced by the time-varying, frequency selective fading channel. The system shown in Fig. 1<sup>[7,8]</sup>, which can describe a large class of digital communication structures, can be described by

$$\mathbf{z}_k = \mathbf{u}_k \mathbf{y}_k + \mathbf{v}_k \tag{1}$$

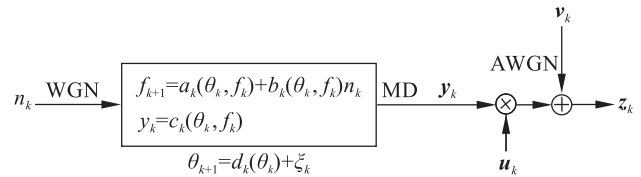


**Fig. 1 Discrete-time model of a digital communication system**

The time difference between the ideal and the actual sampling times is the phase offset denoted by  $\theta_k$ . Then, the timing disturbance can be characterized by the phase offset,  $\theta_k$ , and a frequency drift,  $f_k$ . Thus the MD,  $\mathbf{y}_k$ , can be regarded as an output signal generated by a nonlinear dynamic system with the state variables  $\theta_k$  and  $f_k$ .

## 2 EKF-Based Timing Recovery

### 2.1 EKF algorithm

The state variable in an EKF system relates the state dynamics and the measurements by the following state and measurement equations:

$$\begin{cases} \mathbf{x}_{k+1} = \phi_k(\mathbf{x}_k) + \varphi_k(\mathbf{x}_k)\mathbf{w}_k, \\ \mathbf{z}_k = h_k(\mathbf{x}_k) + \mathbf{v}_k \end{cases} \tag{2}$$

where  $\mathbf{x}_k$  denotes the state vector that may contain many estimated parameters which here is  $\mathbf{x}_k = [\theta_k \ f_k]^T$ ,

The subscript  $k$  is the discrete-time sample index and  $\mathbf{w}_k$  and  $\mathbf{v}_k$  are zero mean, white Gaussian processes.

The structure shown in Fig. 1 exactly fits the signal model for which an EKF is a ‘‘near optimum’’ estimator<sup>[9,10]</sup>, where  $\mathbf{a}_k$ ,  $\mathbf{c}_k$ , and  $\mathbf{d}_k$  are in general, differentiable, nonlinear vector functions and  $\mathbf{b}_k$  is a linear matrix function.

$$\varphi_k(\mathbf{x}_k) = \begin{bmatrix} \mathbf{b}_k(\theta_k, f_k) & \mathbf{0} \\ \mathbf{0} & \mathbf{I} \end{bmatrix} \quad (3)$$

$$\mathbf{h}_k(\mathbf{x}_k) = \mathbf{c}_k(\theta_k, f_k) = \mathbf{y}_k \quad (4)$$

Assume that  $\mathbf{x}_0$  is a Gaussian random variable  $N(\bar{\mathbf{x}}_0, P_0)$  and  $\mathbf{v}_k$  and  $\mathbf{w}_k$  are mutually independent with

$$E[\mathbf{v}_k \mathbf{v}_k^\top] = \mathbf{R}_k, \quad E[\mathbf{w}_k \mathbf{w}_k^\top] = \mathbf{Q}_k \quad (5)$$

Then introduce the matrices

$$\mathbf{F}_k = \left. \frac{\partial \phi_k(\mathbf{x})}{\partial \mathbf{x}} \right|_{\mathbf{x}=\hat{\mathbf{x}}_{k|k}} = \begin{bmatrix} \partial \mathbf{a}_k / \partial f & \partial \mathbf{a}_k / \partial \theta \\ \mathbf{0} & \mathbf{d}_k / \mathbf{d} \theta \end{bmatrix} \quad (6)$$

$$\mathbf{H}_k^\top = \left. \frac{\partial h_k(\mathbf{x})}{\partial \mathbf{x}} \right|_{\mathbf{x}=\hat{\mathbf{x}}_{k|k-1}} = [\partial \mathbf{c}_k / \partial f \quad \partial \mathbf{c}_k / \partial \theta]_{\mathbf{x}=\hat{\mathbf{x}}_{k|k-1}} \quad (7)$$

$$\mathbf{G}_k = g_k(\hat{\mathbf{x}}_{k|k}) = \begin{bmatrix} \mathbf{b}_k(\hat{\theta}_{k|k}, \hat{f}_{k|k}) & \mathbf{0} \\ \mathbf{0} & \mathbf{I} \end{bmatrix} \quad (8)$$

The nonlinear model denoted by Eq. (2) can be approximated to linear equations that conform to the Kalman filtering algorithm by Taylor expansions about the conditional means  $\hat{\mathbf{x}}_{k|k}$  and  $\hat{\mathbf{x}}_{k|k-1}$ . The linearized result can be thought of as a suboptimal algorithm in a minimum mean square error (MMSE) sense to the estimate of  $\mathbf{x}_k$ . Neglecting the second and higher order terms gives a linear approximation of Eq. (2) by the following linear model,

$$\begin{cases} \mathbf{x}_{k+1} = \mathbf{F}_k \mathbf{x}_k + \mathbf{G}_k \mathbf{w}_k + \mathbf{q}_{k,x}, \\ \mathbf{z}_k = \mathbf{H}_k^\top \mathbf{x}_k + \mathbf{v}_k + \mathbf{q}_{k,z} \end{cases} \quad (9)$$

with known, external insertions

$$\mathbf{q}_{k,x} = \phi_k(\hat{\mathbf{x}}_{k|k}) - \mathbf{F}_k \hat{\mathbf{x}}_{k|k} \quad (10)$$

$$\mathbf{q}_{k,z} = h_k(\hat{\mathbf{x}}_{k|k-1}) - \mathbf{H}_k^\top \hat{\mathbf{x}}_{k|k-1} \quad (11)$$

Note that  $\phi_k$  and  $h_k$  are linearized at each time step.

The EKF initialization and recursion are given as

$$\begin{cases} \hat{\mathbf{x}}_{0|0} = E[\mathbf{x}_0] = \bar{\mathbf{x}}_0, \\ \boldsymbol{\Sigma}_{0|0} = E[(\mathbf{x}_0 - \bar{\mathbf{x}}_0)(\mathbf{x}_0 - \bar{\mathbf{x}}_0)^\top] = \mathbf{P}_0 \end{cases} \quad (12)$$

$$\boldsymbol{\Omega}_k = \mathbf{H}_k^\top \boldsymbol{\Sigma}_{k|k-1} \mathbf{H}_k + \mathbf{R}_k \quad (13)$$

$$\mathbf{L}_k = \boldsymbol{\Sigma}_{k|k-1} \mathbf{H}_k \boldsymbol{\Omega}_k^{-1} \quad (14)$$

$$\begin{cases} \hat{\mathbf{x}}_{k|k} = \hat{\mathbf{x}}_{k|k-1} + \mathbf{L}_k (\mathbf{z}_k - h_k(\hat{\mathbf{x}}_{k|k-1})), \\ \hat{\mathbf{x}}_{k+1|k} = \phi_k(\hat{\mathbf{x}}_{k|k}) \end{cases} \quad (15)$$

$$\boldsymbol{\Sigma}_{k|k} = \boldsymbol{\Sigma}_{k|k-1} - \boldsymbol{\Sigma}_{k|k-1} \mathbf{H}_k \boldsymbol{\Omega}_k^{-1} \mathbf{H}_k^\top \boldsymbol{\Sigma}_{k|k-1} \quad (16)$$

$$\boldsymbol{\Sigma}_{k+1|k} = \mathbf{F}_k \boldsymbol{\Sigma}_{k|k} \mathbf{F}_k^\top + \mathbf{G}_k \mathbf{Q}_k \mathbf{G}_k^\top \quad (17)$$

where  $\mathbf{L}_k$  are the Kalman gains which can be pre-computed and stored,  $\hat{\mathbf{x}}_{k|k-1}$  is a prior state estimate,  $\hat{\mathbf{x}}_{k|k}$  is a posterior estimate, and  $\boldsymbol{\Sigma}_{k|k-1}$  and  $\boldsymbol{\Sigma}_{k|k}$  are a prior and posterior error covariance matrices.

## 2.2 EKF estimate of the phase offset

The EKF approach for the timing recovery by estimating the phase offset,  $\theta_k$ , can be described by

$$\begin{bmatrix} \theta_{k+1} \\ f_{k+1} \end{bmatrix} = \begin{bmatrix} 1 & 1 \\ 0 & 1 \end{bmatrix} \begin{bmatrix} \theta_k \\ f_k \end{bmatrix} + \begin{bmatrix} \mathbf{w}_k^\theta \\ \mathbf{w}_k^f \end{bmatrix} \quad (18)$$

$$\mathbf{z}_k = \begin{bmatrix} z_k^I \\ z_k^Q \end{bmatrix} = \begin{bmatrix} u_k^I & -u_k^Q \\ u_k^Q & u_k^I \end{bmatrix} \begin{bmatrix} \cos \theta_k \\ \sin \theta_k \end{bmatrix} + \begin{bmatrix} v_k^I \\ v_k^Q \end{bmatrix} \quad (19)$$

where  $u_k^I$  and  $u_k^Q$  are the transmitted in-phase (I) and quadrature (Q) components. The system observations,  $z_k^I$  and  $z_k^Q$ , are the I and Q components of the output signals with a timing misalignment between the transmitter and the receiver<sup>[11,12]</sup>.

The estimate of  $\theta_k$  without frequency variations is

$$\theta_{k+1} = \theta_k + f_k + \mathbf{w}_k^\theta \quad (20)$$

The estimation of  $f_k$  is

$$\hat{f}_k = \hat{f}_{k-1} + \mathbf{K}_f \text{Im} \{ \mathbf{z}_k e^{-j\hat{\theta}_{k|k-1}} (\hat{u}_k^I + j\hat{u}_k^Q)^* \} \quad (21)$$

where  $\mathbf{K}_f$  is the step size controlling the convergence rate of the input estimation algorithm,  $\text{Im}$  denotes the imaginary part of the underlying argument, the term  $\mathbf{z}_k e^{-j\hat{\theta}_{k|k-1}}$  represents the rotating signal,  $\mathbf{z}_k$ , with a phase angle  $-\hat{\theta}_{k|k-1}$ ,  $\hat{u}_k^I + j\hat{u}_k^Q$  is the  $k$ -th transmitted data symbol obtained by the decision-aided data, and the symbol  $*$  takes the complex conjugate operation of its argument.

The EKF equations for updating state estimates are

$$\begin{cases} \hat{\theta}_{k|k} = \hat{\theta}_{k|k-1} + \mathbf{L}_k \left\{ \begin{bmatrix} z_k^I \\ z_k^Q \end{bmatrix} - \begin{bmatrix} \hat{u}_k^I & -\hat{u}_k^Q \\ \hat{u}_k^Q & \hat{u}_k^I \end{bmatrix} \begin{bmatrix} \cos \hat{\theta}_{k|k-1} \\ \sin \hat{\theta}_{k|k-1} \end{bmatrix} \right\}, \\ \hat{\theta}_{k+1|k} = \hat{\theta}_{k|k} + \hat{f}_k \end{cases} \quad (22)$$

where  $\mathbf{L}_k$  is the Kalman gain and the error covariance updates are obtained from Eqs. (16) and (17), where the parameters vary as the following.

$$\mathbf{F}_k = \left. \frac{\partial \phi_k(\mathbf{x})}{\partial \mathbf{x}} \right|_{\mathbf{x}=\hat{\theta}_{k|k}} = 1, \quad G_k = g_k(\hat{\theta}_{k|k}) = 1 \quad (23)$$

$$\mathbf{H}_k^\top = \left. \frac{\partial h_k(\mathbf{x})}{\partial \mathbf{x}} \right|_{\mathbf{x}=\hat{\theta}_{k|k-1}} = \begin{bmatrix} -\hat{u}_k^I \sin \hat{\theta}_{k|k-1} - \hat{u}_k^Q \cos \hat{\theta}_{k|k-1} \\ -\hat{u}_k^Q \sin \hat{\theta}_{k|k-1} + \hat{u}_k^I \cos \hat{\theta}_{k|k-1} \end{bmatrix} \quad (24)$$

where the symbol  $\hat{u}_k^1 + j\hat{u}_k^Q$  is the estimation of the transmitted symbol which is unknown at the receiver, but which can be obtained using the decision-aided approach from the output of the hard-decision device. Thus, the state update in Eq. (22) can be rewritten as

$$\hat{\theta}_{k|k} = \hat{\theta}_{k|k-1} + \mathbf{L}_k \left\{ \begin{bmatrix} z_k^1 \\ z_k^Q \end{bmatrix} - \begin{bmatrix} \hat{u}_k^1 & -\hat{u}_k^Q \\ \hat{u}_k^Q & \hat{u}_k^1 \end{bmatrix} \begin{bmatrix} \cos \hat{\theta}_{k|k-1} \\ \sin \hat{\theta}_{k|k-1} \end{bmatrix} \right\} \quad (25)$$

In conclusion, Eqs. (12) - (17) and (22) - (25) form the EKF algorithm for adaptive estimation of the phase offset.

### 3 Numerical Experiments

The timing recovery method was simulated for a wavelet packet transform-based multicarrier modulation communication system<sup>[13]</sup> with  $N=64$  subcarriers, a carrier frequency  $f_c = 900$  MHz, a channel bandwidth  $W=5$  MHz, a subcarrier bandwidth  $\Delta f = W/N = 78.125$  kHz, a symbol width  $T_s = \frac{1}{\Delta f} = 12.8$   $\mu$ s, a

wavelet packet basis function of db4, a maximum Doppler frequency  $f_m = 300$  Hz which is quite large, multi-path channels number  $L = 4$ , and delaying times of  $\tau_i = i/(K\Delta f), i = 0, 1, 2, 3$ . All of the test data was modulated by 4QAM.

The pre-computed Kalman phase gains for the KF and EKF schemes are shown in Fig. 2, where  $T_b$  is the nominal bit interval. The initial error covariance was set to  $5/3$  for the phase and  $0.2$  for the frequency. The measurement noise variance was set to  $0.1$  and the noise variances of the random phase and frequency disturbances were set to  $1 \times 10^{-3}$  and  $1 \times 10^{-4}$ . Note that the EKF gains are oscillating due to the nonlinear function  $h_k(x_k)$  in Eq. (4) and converge faster than

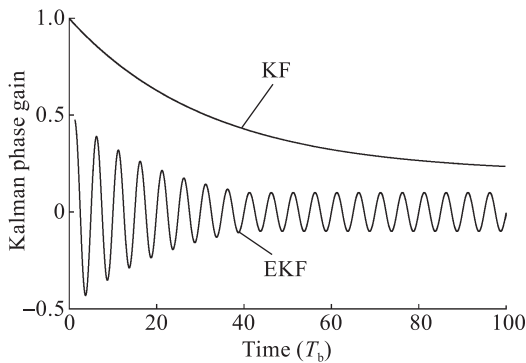


Fig. 2 Pre-computed Kalman phase gains for the KF and EKF schemes

the KF gains, because they are updated every time step, while the KF gains are smooth since they are updated only every four time steps.

The validity of the method was investigated for two types of channel models.

#### Model I: AWGN channel model

This simulation compares the timing recovery of the current algorithm with those of several conventional methods. The step size in Eq. (21) was set to  $K_f = 2^{-10}$  to achieve stable fast convergence for this simulation environment.

Figure 3 shows the RMS error of the phase offset estimates for the PLL, ML, KF, and EKF schemes. The RMS error of the EKF phase estimation is around  $0.13$  at time  $20T_b$  and  $0.081T_b$  at time  $40$ , which is smaller and converging faster than for the other three methods. The BER performances of the PLL, ML, KF, and EKF schemes for the same channel are shown in Fig. 4, which clearly reflects the efficiency of the EKF algorithm over the other three methods. For example, the

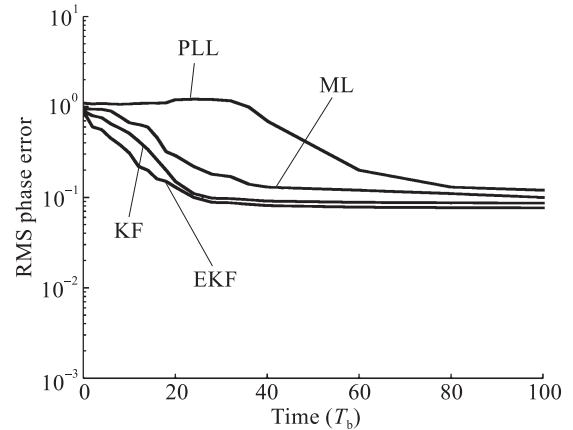


Fig. 3 RMS phase error for AWGN channel

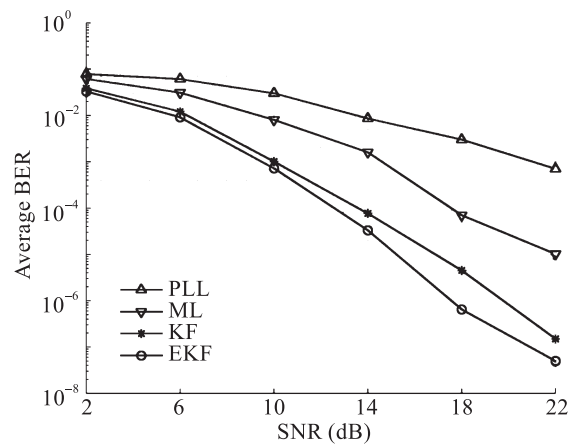


Fig. 4 Average BER versus SNR for AWGN channel

minimum BER of the EKF scheme is  $0.5 \times 10^{-7}$  dB for a signal noise ratio (SNR) of 22 dB.

### Model II: Rayleigh fading channel model

A Rayleigh fading channel model with variable channel coefficients was also used to test the efficiency of the decision-aided EKF algorithm over the other scheme. The settings are the same in model I. The result in Fig. 5 shows that the RMS error of the EKF phase estimation is around 0.084 at time  $20T_b$  and 0.056 at time  $40T_b$ , less than for the other three methods, with the EKF method having faster convergence in the Rayleigh fading channel. As with model I, Fig. 6 shows that the bit error performance of the decision-aided EKF scheme for the fading channel after time offset is better than for the PLL, ML, and KF schemes. The decision-aided EKF method has a less bit error rate than the PLL, ML, and KF methods for the same SNR, with a BER of  $1.8 \times 10^{-7}$  dB for SNR of 22 dB which is smaller than for the other methods.

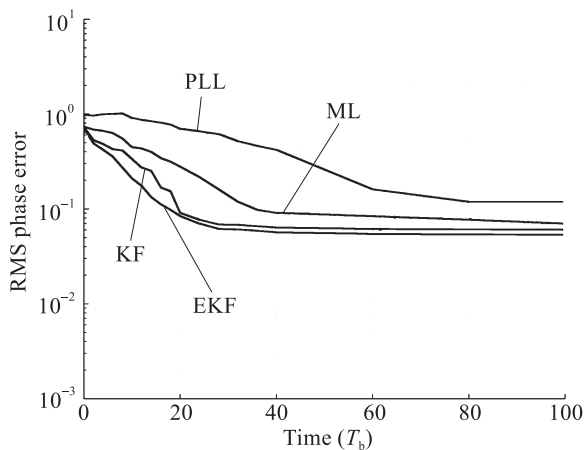


Fig. 5 RMS phase error for Rayleigh channel

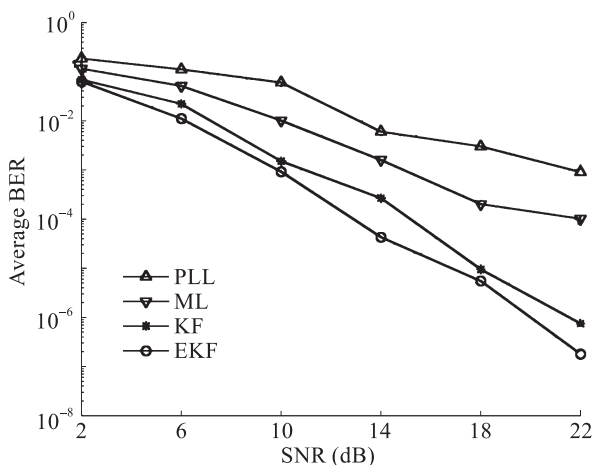


Fig. 6 Average BER versus SNR for Rayleigh channel

## 4 Conclusions

An adaptive timing recovery method was developed based on decision-aided EKF for both AWGN and Rayleigh fading channels in a wavelet packet transform-based multicarrier modulation communication system. The method is compared with the conventional PLL, ML, and KF methods. Simulations show that the decision-aided EKF performs better than the PLL, ML, and KF methods in terms of convergence rate, RMS error, and BER, since the scheme takes into account the nonlinear relationship between the signal samples and timing errors. Offline computations of the Kalman gains reduce the online computations to a level comparable to those used by a conventional PLL. Thus, the decision-aided EKF based timing recovery is much more suitable for the nonlinear time-varying fading channel environment of wavelet packet transform-based multicarrier modulation communication system.

## References

- [1] Lakshmanan M K, Nikookar H. A review of wavelets for digital wireless communication. *Springer Journal on Wireless Personal Communication*, 2006, 37(3-4): 387-420.
- [2] Nikookar H, Lakshmanan M K. Comparison of sensitivity of OFDM and wavelet packet modulation to time synchronization error. In: 19<sup>th</sup> Annual IEEE International Symposium on Personal, Indoor and Mobile Radio Communication. Cannes, France, 2008.
- [3] Padua M S, Deckmann S M, Sperandio G S. Comparative analysis of synchronization algorithms based on PLL, RDFT and Kalman filter. In: IEEE International Symposium on Industrial Electronics. Vigo, Spain, 2007: 964-970.
- [4] Nayak A R, Barry J R, Feyh G, et al. Timing recovery with frequency offset and random walk: Cramér-Rao bound and a phase-locked loop postprocessor. *IEEE Trans. Commun.*, 2006, 54: 2004-2013.
- [5] Kjeldsen E, Lindsey A. Receiver timing recovery for adaptive wavelet packet modulated signals. In: Conference Record of the Thirty-Sixth Asilomar Conference on Signals, Systems and Computers. Asilomar, 2002, 1: 92-96.
- [6] Driessen P F. DPLL bit synchronizer with rapid acquisition using adaptive Kalman filtering technique. *IEEE Trans. Commun.*, 1994, 42(9): 2673-2675.

- [7] Aghamohammadi A, Meyr H, Ascheid G. Adaptive synchronization and channel parameter estimation using an extended Kalman filter. *IEEE Transactions on Communications*, 1989, **37**(11): 1212-1219.
- [8] Liu Jingfeng, Song Hongwei, Vijaya Kumar BVK. Dual segmented Kalman filters based symbol timing recovery for Low-SNR partial response data storage channels. In: Global Telecommunications Conference. San Francisco, USA, 2003: 4084-4090.
- [9] Anderson B D, Moore J B. Optimal Filtering. Englewood Cliffs, NJ: Prentice-Hall, 1979.
- [10] Julier S J, Uhlmann J K. A new extension of the Kalman filter to nonlinear systems. In: 11th Int. Symp. Aerospace/Defence Sensing, Simulation, Controls. <http://citeseer.ist.psu.edu/julier97new.html>, 1997.
- [11] Welch G, Bishop G. An introduction to the Kalman filter. [http://www.cs.unc.edu/~welch/media/pdf/kalman\\_intro.pdf](http://www.cs.unc.edu/~welch/media/pdf/kalman_intro.pdf), 2004.
- [12] Lin Wei-Tsen, Chang Dah-Chung. Adaptive carrier synchronization using decision-aided Kalman filtering algorithms. *IEEE Transactions on Consumer Electronics*, 2007, **53**(4): 1260-1267.
- [13] Hao Jiuyu, Wang Ke, Wang Xiaomei, et al. Implementation of wavelet packet transform-based multicarrier communication system. *Journal of Tianjin University*, 2007, **40**(1): 24-27. (in Chinese)